Multiuser Detection for Out-of-Cell Cochannel Interference Mitigation in the IS–95 Downlink

D. Richard Brown III, H. Vincent Poor, Sergio Verdú, and C. Richard Johnson, Jr.

This research was supported in part by NSF grants ECS-9811297, ECS-9811095, EEC-9872436, and Applied Signal Technology. D.R. Brown III is with the Department of Electrical and Computer Engineering, Worcester Polytechnic Institute, Worcester, MA 01609, USA. H.V. Poor and S. Verdú are with the Department of Electrical Engineering, Princeton University, Princeton, NJ 08544 USA. C.R. Johnson, Jr. is with the School of Electrical Engineering, Cornell University, Ithaca, NY 14853 USA.

Abstract

This paper considers the application of multiuser detection techniques to improve the quality of downlink reception in a multi-cell IS–95 digital cellular communication system. In order to understand the relative performance of suboptimum multiuser detectors including the matched filter detector, optimum multiuser detection in the context of the IS–95 downlink is first considered. A reduced complexity optimum detector that takes advantage of the structural properties of the IS–95 downlink and exhibits exponentially lower complexity than the brute-force optimum detector is developed. The Group Parallel Interference Cancellation (GPIC) detector, a suboptimum, low-complexity multiuser detector that also exploits the structure of the IS–95 downlink is then developed. Simulation evidence is presented that suggests that the performance of the GPIC detector may be near-optimum in several cases. The GPIC detector is also tested on a snapshot of on-air data measured with an omnidirectional antenna in an active IS–95 system and is shown to be effective for extracting weak downlink transmissions from strong out-of-cell cochannel interference. The results of this paper suggest that the GPIC detector offers the most performance gain in scenarios where weak downlink signals are corrupted by strong out-of-cell cochannel interference.

I. Introduction

An important milestone in the development of personal wireless communication systems occurred in the early 1990's when Qualcomm introduced a new digital cellular communication system based on Code Division Multiple Access (CDMA) technology. The proposed cellular system offered several advantages over first generation analog cellular systems including increased capacity and reliability as well as improved sound quality and battery life. Early trials of this new cellular system proved to be quite successful and, in 1993, the details of the system were published by the Telecommunications Industry Association as the IS–95A standard [1].

Despite the well documented performance benefits of multiuser detection in the literature prior to 1993, the IS–95 cellular standard was designed such that adequate performance could be achieved by a downlink receiver (typically a mobile handset) using conventional single-user matched filter detection with coherent multipath combining. The choice of matched filter detection for the IS–95 downlink resulted in the need for strict, closed-loop power control on both the uplink and downlink in order to avoid "near-far" problems (cf. [2]). One reason for this approach is that, unlike power control, the majority of the multiuser detectors proposed in the literature have been regarded as too complex for cost-effective implementation in IS–95 downlink receivers. Despite the exponential perfor-

mance improvements in microprocessors and DSPs over the last decade, these constraints have continued to outweigh the potential performance benefits of multiuser detection for the IS–95 downlink.

In this paper we attempt to bridge some of the gap between IS–95 and multiuser detection. Toward that goal, several authors have studied the problem of improving the performance of IS-95 and third generation Wideband-CDMA downlink reception in a *single-cell* environment. In [3]–[12] the authors observe that the orthogonality of the user transmissions within a particular cell is destroyed by multiple paths in the propagation channel between the base station and the IS–95 downlink receiver. The authors propose receivers that all share the common feature of a linear equalizer front-end that cancels the effects of the multipath propagation channel and restores the orthogonality of the users. This approach effectively eliminates the in-cell multiuser interference and allows the conventional matched filter detector to be used. In [13], the authors propose and compare several algorithms applicable to the IS–95 downlink for multipath channel estimation. In [14], [15], the authors developed a nonlinear multipath canceller to cancel the in-cell multiuser interference caused by multipath replicas of the base station's pilot signal.

Our approach here differs from the prior approaches in that we investigate multiuser detection for the IS–95 downlink in a *multi-cell* environment. Multiuser detection in a multi-cell environment was considered recently for the IS–95 uplink in [16], [17]. In this paper we consider receivers that mitigate the effects of the out-of-cell cochannel interference from neighboring base stations in the IS–95 downlink. To establish a performance benchmark, we first examine optimum detection for the IS–95 downlink and develop a reduced complexity optimum detector that exploits the structure of the IS–95 downlink. We then propose the Group Parallel Interference Cancellation (GPIC) detector, a suboptimum, low-complexity multiuser detector that also exploits the structure of the IS–95 downlink.

The results of this paper suggest that multiuser detection may provide modest performance improvements over the conventional matched filter detector in scenarios where a strong desired signal is corrupted by weak out-of-cell cochannel interference. On the other hand, our results suggest that multiuser detection may offer significant performance

improvements in conditions where an IS–95 downlink receiver is detecting a weak desired signal in the presence of strong out-of-cell cochannel interference. Although this scenario would be unusual for a subscribing user in an IS–95 cellular system, the practical implications of our results include:

- Nonsubscribing users (e.g. eavesdroppers or test/diagnostic receivers) which do not have the benefit of power control may wish to extract a weak desired signal from strong out-of-cell cochannel interference. Multiuser detection receivers tend to offer superior performance in these cases.
- Subscribing users with multiuser detectors require less transmit power from their base station to maintain an equal quality of service. This "good neighbor" effect leads to a reduced level of cochannel interference induced on other out-of-cell users in the system.

This balance of this paper is organized as follows. In Section II we develop a concise model with mild simplifying assumptions for the IS–95 downlink that includes the effects of the time and phase asynchronous, nonorthogonal, and non-cyclostationary transmissions of a M base station communication system. In Section III we use this model to understand optimum multiuser detection in the context of the IS–95 downlink. Although the optimum detector is often too complex for implementation in realistic systems, its role is still important in order to determine the relative performance of suboptimum multiuser detectors. In Section IV we show that the structure of the IS–95 downlink allows the optimum detector to be posed in a computationally efficient form with complexity exponentially less than a brute-force implementation. In Section V we develop a computationally efficient nonlinear multiuser detector for the IS–95 downlink called the Group Parallel Interference Cancellation (GPIC) detector. The GPIC detector is derived from examination of properties of the reduced complexity optimum detector and also exploits the structure in the IS–95 downlink. In Section VI we examine the performance of the GPIC detector relative to the conventional matched filter and optimum detectors via simulation and show that the GPIC detector exhibits near-optimum performance in the cases examined and provides the largest benefit when the desired signal is received in the presence of strong out-of-cell cochannel interference. Finally, in Section VII we apply the GPIC detector to a snapshot

of on-air data from an active IS–95 system and present results that suggest that GPIC detection offers significant performance improvements when extracting weak signals in the presence of severe out-of-cell cochannel interference.

II. IS–95 Downlink System Model

Figure 1 shows a model of a single IS–95 base station downlink transmitter. This model is simplified in the sense that the scrambling and channel encoding operations specified by the IS–95 standard prior to the channelization block in Figure 1 are not shown. An IS–95 downlink receiver typically consists of four fundamental stages: multipath timing and phase estimation (via the downlink pilot), coded symbol detection (matched filter with multipath combining), decoding (convolutional and repetition), and descrambling. Since this paper focuses on the problem of improving the performance of the detection stage, we consider the portion of the IS–95 downlink transmitter "inside the coders" as shown in Figure 1.

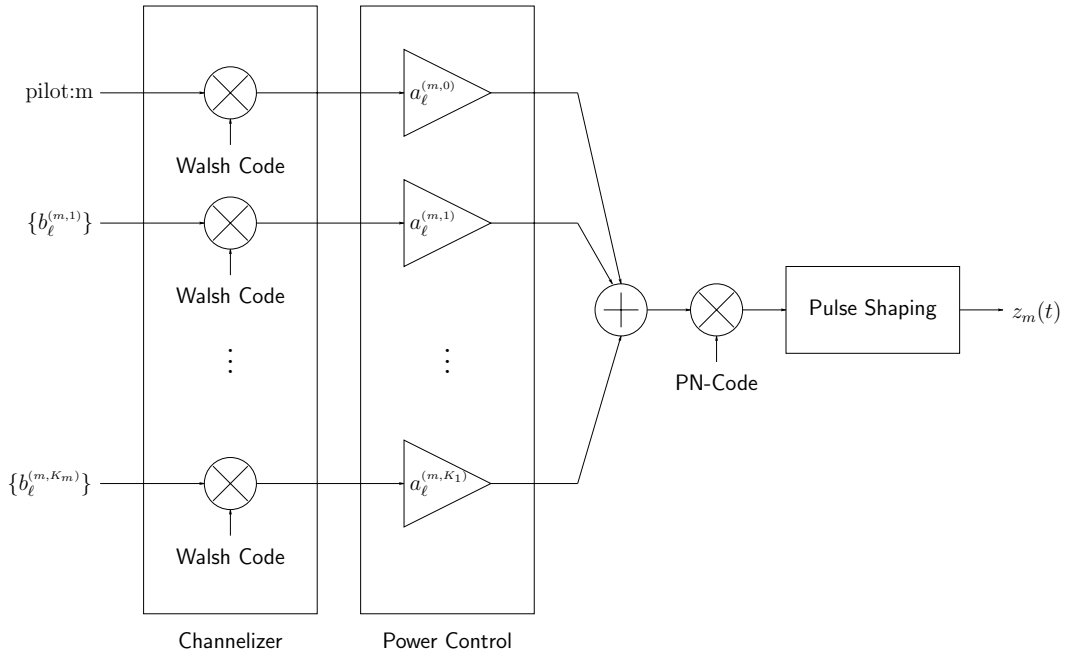

Fig. 1. Single base station IS–95 downlink baseband transmitter model.

We denote m as the base station index and K_m as the number of data streams simultaneously transmitted by the m^{th} base station, not including the pilot transmission. Note

that K_m is typically greater than the actual number of physical users in the cell since the IS–95 standard specifies that each base station must transmit additional data streams for call setup, paging, and overhead information. For the purposes of this paper, we will henceforth refer to each of these data streams as a "user" even if the data stream is an overhead channel and not actually allocated to a particular user in the cell. The details of Figure 1 as specified by the IS–95 standard may be summarized as follows:

- Channelizer: Orthogonalizes the user transmissions by assigning a unique length-64 Walsh code to each user and spreads the input symbols with this code. Each user's Walsh code remains fixed for the duration of their connection. The Walsh-0 code is always assigned to the base station's pilot signal which transmits a constant stream of binary symbols equal to +1. The remaining 63 Walsh codes are assigned as needed to the users in the cell as well as to overhead and paging channels.
- Power Control: Sets the gain on each user's transmission to provide a minimum acceptable transmission quality in order to avoid generating excessive cochannel interference in neighboring cells.
- PN-Code: Multiplies the chip-rate aggregate base station data stream by a complex pseudonoise (PN) code in order to cause the cochannel interference observed by the users in neighboring cells to appear noiselike and random [18, pp. 11]. Each base station uses the same PN-code but is distinguished by a unique, fixed PN-phase. The PN-code has elements from the set $\{1+j, 1-j, -1+j, -1-j\}$ and has a period of 2^{15} chips.
- Pulse Shaping: Specified in the IS–95 standard.

Note that the total spreading gain on the coded symbols in the IS–95 downlink is 64 and that all spreading occurs in the channelizer block. The PN-code does not provide any additional spreading.

Since the IS–95 standard specifies universal frequency reuse for all base stations in a cellular system, it is reasonable to model the downlink receiver's observation as the sum of transmissions from M base stations and additive channel noise as shown in Figure 2. Each base station's aggregate transmission passes through an individual propagation channel

that accounts for the effects of multipath, delay, and attenuation. The channel noise is modeled as an additive, white, complex Gaussian random process denoted by $\sigma w(t)$ where $E(w(t)) = 0$ and $E(\mathrm{Re}(w(t))^2) = E(\mathrm{Im}(w(t))^2) = 1/2$. The real and imaginary parts are uncorrelated and also assumed to be independent of the base station transmissions.

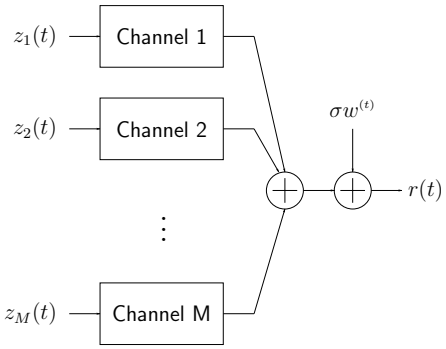

Fig. 2. Baseband IS–95 downlink received signal model.

We define the total number of users in the system as $K = \sum_{m=1}^{M} K_m$. To facilitate the analytical development in the following sections, we also make the following simplifying assumptions which may be relaxed or eliminated at the expense of greater notational complexity:

- We ignore the soft-handoff feature of IS–95 where two base stations may be transmitting identical bit streams to a single user.
- We assume the user population remains fixed over the receiver's observation interval. This implies that users do not enter or leave the system, users are not handed off between cells, and that voice activity switching does not occur during the observation interval.
- We ignore base station antenna sectorization.

Indexing the users by a two dimensional index (base station, user number), we denote the $(m,k)^{\text{th}}$ user's positive real amplitude and coded binary symbol at symbol index ℓ as $a_\ell^{(m,k)}$ and $b_\ell^{(m,k)}$ respectively. We denote the unit-energy normalized combined impulse response of the $(m,k)^{\text{th}}$ user's channelization code, PN-code, baseband pulse shaping, and propagation channel at symbol index ℓ as $s_\ell^{(m,k)}(t)$. Note that $s_\ell^{(m,k)}(t)$ includes any inherent

propagation delay and asynchronicity between base stations and is assumed to be FIR. We also denote ϕ_m as the received phase of the transmission from the m^{th} base station. The baseband signal observed at the downlink receiver may then be written as

$$r(t) = \sum_{m=1}^{M} e^{j\phi_m} \sum_{\ell=-L}^{L} \left[a_\ell^{(m,0)} s_\ell^{(m,0)}(t-\ell T) + \sum_{k=1}^{K_m} b_\ell^{(m,k)} a_\ell^{(m,k)} s_\ell^{(m,k)}(t-\ell T) \right] + \sigma w(t).$$

where we have separated the terms corresponding to the non-data-bearing pilots with the superscript notation $(m,0)$.

In order to represent the observation $r(t)$ compactly, we establish the following vector notation. If $x_\ell^{(m,k)}$ represents a (possibly complex) scalar quantity corresponding to the $(m,k)^{\text{th}}$ user at symbol index ℓ, we can construct the vectors

$$\begin{aligned} \boldsymbol{x}_\ell^{[m]} &= \left[x_\ell^{(m,1)}, \ldots, x_\ell^{(m,K_m)}\right]^\top, \\ \boldsymbol{x}^{[m]} &= \left[\boldsymbol{x}_{-L}^{[m]\top}, \ldots, \boldsymbol{x}_{L}^{[m]\top}\right]^\top, \text{ and} \\ \boldsymbol{x} &= \left[\boldsymbol{x}^{[1]\top}, \ldots, \boldsymbol{x}^{[M]\top}\right]^\top. \end{aligned}$$

The superscripts $\boldsymbol{x}^\top$, $\boldsymbol{x}^*$ and $\boldsymbol{x}^H$ denote transpose, complex conjugate, and complex conjugate transpose, respectively. Define $\boldsymbol{a}$ and $\boldsymbol{b}$ according to this notation and define the vector of signature waveforms as

$$\begin{aligned} \boldsymbol{s}_\ell^{[m]}(t-\ell T) &= \left[s_\ell^{(m,1)}(t-\ell T), \ldots, s_\ell^{(m,K_m)}(t-\ell T)\right]^\top, \\ \boldsymbol{s}^{[m]}(t) &= \left[\boldsymbol{s}_{-L}^{[m]\top}(t+LT), \ldots, \boldsymbol{s}_{L}^{[m]\top}(t-LT)\right]^\top, \text{ and} \\ \boldsymbol{s}(t) &= \left[\boldsymbol{s}^{[1]\top}(t), \ldots, \boldsymbol{s}^{[M]\top}(t)\right]^\top. \end{aligned}$$

Finally, define

$$\boldsymbol{A} = \operatorname{diag}\left(\left[e^{j\phi_1}\boldsymbol{a}^{[1]\top}, \ldots, e^{j\phi_M}\boldsymbol{a}^{[M]\top}\right]^\top\right)$$

as the $K(2L+1) \times K(2L+1)$ dimensional diagonal matrix of user amplitudes multiplied by the appropriate base station transmission phases. We can then write the continuous time observation as

$$\begin{aligned} r(t) &= \underbrace{\sum_{m=1}^{M} e^{j\phi_m} \sum_{\ell=-L}^{L} a_\ell^{(m,0)} s_\ell^{(m,0)}(t-\ell T)}_{\text{pilots}} + \underbrace{\boldsymbol{s}^\top(t)\boldsymbol{A}\boldsymbol{b}}_{\text{users}} + \underbrace{\sigma w(t)}_{AWGN} \\ &= p(t) + \boldsymbol{s}^\top(t)\boldsymbol{A}\boldsymbol{b} + \sigma w(t) \end{aligned} \tag{1}$$

where the pilots are denoted as $p(t)$ for notational convenience.

III. Optimum Detection

In this section we examine optimum (joint maximum likelihood) detection in the context of the previously developed IS–95 downlink system model. In a single-cell scenario with single-path channels, an IS–95 downlink receiver observes the sum of K orthogonally modulated signals in the presence of independent AWGN. It is easy to show that the optimum detector is equivalent to the conventional single-user matched filter detector in this case. In this paper, however, we consider the multi-cell scenario where an IS–95 downlink receiver observes nonorthogonal out-of-cell cochannel interference and the optimum detector is not the matched filter detector.

We assume that the receiver is able to acquire the pilot (and hence the PN-phase) of each base station $m \in \{1, \ldots, M\}$ via correlation with the known periodic PN-code of length 2^{15}. This then allows the receiver to estimate the impulse response of the propagation channel and transmission phases of each base station. For each base station, the receiver can then construct a bank of 63 matched filters, one matched filter for each of the non-pilot Walsh codes, in order to determine which users are active in each cell. Since the receiver now knows the Walsh codes of the active users, the phase of the PN-code, the propagation channels, and the baseband pulse-shaping, we can construct the set of $s_\ell^{(m,k)}(t)$ for all users in the multi-cell system. Finally, amplitude estimates are generated for each user and the pilots (cf. [19]). For the purposes of the remaining analytical development, we assume that all of these estimates are perfect and that the only unknowns in (1) are $\boldsymbol{b}$ and $\sigma w(t)$.

Let $\mathcal{I}$ represent a compact interval in time containing the support of $r(t)$ and let $\mathcal{U}$ represent the set of cardinality $2^{K(2L+1)}$ containing all admissible binary symbol vectors of length $K(2L+1)$. Then the jointly optimum symbol estimates [20] are given by

$$\hat{\boldsymbol{b}}_{\mathsf{OPT}} = \arg\max_{\boldsymbol{u}\in\mathcal{U}} \exp\left(-\frac{1}{\sigma^2}\int_{\mathcal{I}} |r(t) - p(t) - \boldsymbol{s}^\top(t)\boldsymbol{A}\boldsymbol{u}|^2 dt\right).$$

Manipulation of the term inside the exponent yields the expression for jointly optimum IS–95 downlink symbol estimates as

$$\hat{\boldsymbol{b}}_{\mathsf{OPT}} = \arg\max_{\boldsymbol{u}\in\mathcal{U}} \underbrace{2\mathrm{Re}[\boldsymbol{u}^\top \boldsymbol{A}^H(\boldsymbol{y}-\boldsymbol{p})] - \boldsymbol{u}^\top \boldsymbol{A}^H \boldsymbol{R}\boldsymbol{A}\boldsymbol{u}}_{\Omega(\boldsymbol{u})}$$

where $\boldsymbol{y} = \int_{\mathcal{I}} \boldsymbol{s}^*(t) r(t)\, dt$ represents the $K(2L+1)$-vector of matched filter outputs, $\boldsymbol{p} = \int_{\mathcal{I}} \boldsymbol{s}^*(t) p(t)\, dt$ represents the $K(2L+1)$-vector of matched filter outputs for the pilot portion of the received signal, and $\boldsymbol{R} = \int_{\mathcal{I}} \boldsymbol{s}^*(t) \boldsymbol{s}^\top(t)\, dt$ represents the $K(2L+1) \times K(2L+1)$ dimensional user signature correlation matrix.

The brute-force solution to the problem of computing the jointly optimum symbol estimates requires the exhaustive computation of $\Omega(\boldsymbol{u})$ over the set of all $2^{K(2L+1)}$ hypotheses $\boldsymbol{u} \in \mathcal{U}$ to find the maximum.

IV. Reduced Complexity Optimum Detection

In this section we take advantage of the structure of the IS–95 downlink in order to propose an *optimum* detector that exhibits significantly less complexity than the brute-force approach. The intuitive idea behind the reduced complexity optimum detector is to use the fact that the $K_m + 1$ synchronous user plus pilot transmissions from base station m are mutually orthogonal at every symbol index if the propagation channel from the m^{th} base station to the receiver is single-path. This will allow us to "decouple" the decisions of one base station's users to achieve the desired complexity reduction while retaining optimality. This idea can also be applied in the multipath channel case but since users within a cell are no longer orthogonal there will be some loss of optimality. Note that even if the orthogonality between the users within a particular cell is restored using the equalization techniques described in [3], [4], [5], [6], [7], [8], [9], [10], [11], the resulting matched filter bank outputs will contain noise terms that are correlated across the users. Hence, the ideas described in this section may also be applied to an IS–95 downlink receiver with an equalizer front-end but there will be some loss of optimality.

To develop the reduced complexity optimum detector, we first observe that the signature correlation matrix exhibits the structure

$$\boldsymbol{R} = \int_{\mathcal{I}} \begin{bmatrix} \boldsymbol{s}^{[1]*}(t) \\ \vdots \\ \boldsymbol{s}^{[M]*}(t) \end{bmatrix} \begin{bmatrix} \boldsymbol{s}^{[1]\top}(t) & \cdots & \boldsymbol{s}^{[M]\top}(t) \end{bmatrix} dt = \begin{bmatrix} \boldsymbol{R}^{[1,1]} & \cdots & \boldsymbol{R}^{[1,M]} \\ \vdots & \ddots & \vdots \\ \boldsymbol{R}^{[M,1]} & \cdots & \boldsymbol{R}^{[M,M]} \end{bmatrix}$$

where $\boldsymbol{R}^{[m,m']}$ has dimension $K_m(2L+1) \times K_{m'}(2L+1)$. The submatrices $\boldsymbol{R}^{[m,m']}$ have the

structure

$$\boldsymbol{R}^{[m,m']} = \begin{bmatrix} \boldsymbol{R}^{[m,m']}_{-L,-L} & \cdots & \boldsymbol{R}^{[m,m']}_{-L,L} \\ \vdots & \ddots & \vdots \\ \boldsymbol{R}^{[m,m']}_{L,-L} & \cdots & \boldsymbol{R}^{[m,m']}_{L,L} \end{bmatrix}$$

where

$$\boldsymbol{R}^{[m,m']}_{\ell,\ell'} = \int_{\mathcal{I}} \boldsymbol{s}^{[m]*}_{\ell}(t)\boldsymbol{s}^{[m']\top}_{\ell'}(t)\,dt = \boldsymbol{R}^{[m',m]H}_{\ell',\ell}.$$

At this point we require the propagation channels to be single-path in order to proceed with the complexity reduction. This assumption, combined with the facts that

1. the IS–95 pulse shaping filters approximately satisfy the Nyquist pulse criterion and
2. each base station assigns orthonormal signature waveforms to the set of users in its cell,

implies that the downlink transmissions in each cell do not interfere with the other downlink transmissions in the same cell and that the downlink transmissions in each cell are received without any intersymbol interference. In this case, the IS–95 downlink signature correlation matrix exhibits two special properties:

1. The lack of intersymbol interference implies that $\boldsymbol{R}^{[m,m]}_{\ell,\ell'} = \boldsymbol{0}$ for $\ell \neq \ell'$.
2. The orthonormal signature sequences of all in-cell users of each base-station at symbol index ℓ implies that $\boldsymbol{R}^{[m,m]}_{\ell,\ell} = \boldsymbol{I}$.

The combination of these two properties implies that $\boldsymbol{R}^{[m,m]} = \boldsymbol{I}$ for $m = 1, \ldots, M$. Let $\boldsymbol{H} = \boldsymbol{A}^H\boldsymbol{R}\boldsymbol{A}$ and note that since $\boldsymbol{R}$ is a Hermitian matrix then $\boldsymbol{H}$ is also Hermitian. Moreover, since $\boldsymbol{A}$ is diagonal, $\boldsymbol{H}$ shares the same IS–95 structure properties as $\boldsymbol{R}$ except that

$$\boldsymbol{H}^{[m,m]} = \boldsymbol{A}^{[m,m]H}\boldsymbol{A}^{[m,m]} \tag{2}$$

It turns out that this difference will not matter in the maximization of $\Omega(\boldsymbol{u})$. Using our previously developed notation, we can write

$$\Omega(\boldsymbol{u}) \;=\; 2\mathrm{Re}\big[\boldsymbol{u}^\top\boldsymbol{A}^H(\boldsymbol{y}-\boldsymbol{p})\big] - \boldsymbol{u}^\top\boldsymbol{H}\boldsymbol{u}. \tag{3}$$

Since $\boldsymbol{A}$ is diagonal and $\boldsymbol{u}$ is real, we can isolate the symbols from the first[1] base station to write

$$2\mathrm{Re}[\boldsymbol{u}^\top \boldsymbol{A}^H(\boldsymbol{y}-\boldsymbol{p})] \;=\; \boldsymbol{u}^{[1]\top} 2\mathrm{Re}\big[\boldsymbol{A}^{[1]H}(\boldsymbol{y}^{[1]}-\boldsymbol{p}^{[1]})\big] + \bar{\boldsymbol{u}}^\top 2\mathrm{Re}\big[\bar{\boldsymbol{A}}^H(\bar{\boldsymbol{y}}-\bar{\boldsymbol{p}})\big] \qquad (4)$$

where vectors with an overbar are $(K-K_1)(2L+1)\times 1$ dimensional with elements from all base stations except $m=1$ and matrices with an overbar are $(K-K_1)(2L+1)\times(K-K_1)(2L+1)$ dimensional with corresponding elements.

The quadratic term in (3) may be rewritten as

$$\boldsymbol{u}^\top \boldsymbol{H}\boldsymbol{u} = \sum_{m=1}^{M}\sum_{m'=1}^{M} \boldsymbol{u}^{[m]\top}\boldsymbol{H}^{[m,m']}\boldsymbol{u}^{[m']}.$$

The binary nature of $\boldsymbol{u}$ and (2) imply that

$$\begin{aligned}\boldsymbol{u}^{[m]\top}\boldsymbol{H}^{[m,m]}\boldsymbol{u}^{[m]} &= \mathbf{1}^\top \boldsymbol{A}^{[m,m]H}\boldsymbol{A}^{[m,m]}\mathbf{1}\\ &= \alpha_m\end{aligned}$$

where α_m is a real positive constant that does not depend on $\boldsymbol{u}$. Denoting $\alpha=\sum_{m=1}^{M}\alpha_m$, we can then write

$$\boldsymbol{u}^\top \boldsymbol{H}\boldsymbol{u} = \alpha + \sum_{m=1}^{M}\sum_{m'\neq m} \boldsymbol{u}^{[m]\top}\boldsymbol{H}^{[m,m']}\boldsymbol{u}^{[m']}.$$

As before, we isolate the symbols from the first base station to write

$$\boldsymbol{u}^\top \boldsymbol{H}\boldsymbol{u} = \alpha + \sum_{m=2}^{M}\boldsymbol{u}^{[m]\top}\boldsymbol{H}^{[m,1]}\boldsymbol{u}^{[1]} + \sum_{m=2}^{M}\boldsymbol{u}^{[1]\top}\boldsymbol{H}^{[1,m]}\boldsymbol{u}^{[m]} + \underbrace{\sum_{m=2}^{M}\sum_{\substack{m'\neq m\\ m'\neq 1}}\boldsymbol{u}^{[m]\top}\boldsymbol{H}^{[m,m']}\boldsymbol{u}^{[m']}}_{G(\bar{\boldsymbol{u}})}.$$

Since $\boldsymbol{H}$ is a Hermitian matrix then $\boldsymbol{H}^{[m,1]H}=\boldsymbol{H}^{[1,m]}$ and we can write

$$\boldsymbol{u}^\top \boldsymbol{H}\boldsymbol{u} = \alpha + \sum_{m=2}^{M}\boldsymbol{u}^{[1]\top} 2\mathrm{Re}\left(\boldsymbol{H}^{[1,m]}\boldsymbol{u}^{[m]}\right) + G(\bar{\boldsymbol{u}}). \qquad (5)$$

[1]In order to achieve the maximum complexity reduction we assume without loss of generality that $K_1 = \max_m K_m$.

Finally, we plug (4) and (5) back into (3) and collect terms to write

$$\Omega(\boldsymbol{u}) = \boldsymbol{u}^{[1]\top} \underbrace{2\mathrm{Re}\left[\boldsymbol{A}^{[1]H}(\boldsymbol{y}^{[1]} - \boldsymbol{p}^{[1]}) - \sum_{m=2}^{M} \boldsymbol{H}^{[1,m]}\boldsymbol{u}^{[m]}\right]}_{F(\bar{\boldsymbol{u}})} + \bar{\boldsymbol{u}}^{\top} 2\mathrm{Re}\big[\bar{\boldsymbol{A}}^{H}(\bar{\boldsymbol{y}} - \bar{\boldsymbol{p}})\big] - \alpha - G(\bar{\boldsymbol{u}}). \tag{6}$$

Observe that, for any $\bar{\boldsymbol{u}} \in \mathbb{B}^{K-K_1}$, (6) is maximized when $\boldsymbol{u}^{[1]} = \mathrm{sgn}(F(\bar{\boldsymbol{u}}))$. Hence, the reduced complexity optimum detector needs only to compute

$$\hat{\bar{\boldsymbol{b}}}_{\mathsf{OPT}} = \arg \max_{\bar{\boldsymbol{u}} \in \mathbb{B}^{K-K_1}} \Omega\left(\left[\mathrm{sgn}(F(\bar{\boldsymbol{u}}))^{\top}, \bar{\boldsymbol{u}}^{\top}\right]^{\top}\right) \tag{7}$$

from which the vector of optimum symbol estimates can be written directly as

$$\hat{\boldsymbol{b}}_{\mathsf{OPT}} \;=\; \left[\mathrm{sgn}\left(F\left(\hat{\bar{\boldsymbol{b}}}_{\mathsf{OPT}}\right)\right)^{\top}, \hat{\bar{\boldsymbol{b}}}_{\mathsf{OPT}}^{\top}\right].$$

Note that, in contrast to the brute-force optimum detector, (7) only requires the computation of $\Omega(\boldsymbol{u})$ over a set of $2^{(K-K_1)(2L+1)}$ hypotheses in order to find the maximum. For a cell system with two or three significant base stations, this complexity reduction can be significant.

This prior analysis can also be easily applied to the synchronous CDMA case where the brute-force optimum detector requires the evaluation of $\Omega(\boldsymbol{u})$ for 2^K hypotheses. In this case, the reduced complexity optimum detector requires the evaluation of $\Omega(\boldsymbol{u})$ for 2^{K-K_1} hypotheses.

V. Group Parallel Interference Cancellation Detection

In this section, we examine the properties of the reduced complexity optimum detector in order to develop a low-complexity suboptimum detector called the Group Parallel Interference Cancellation (GPIC) detector. Like the reduced complexity optimum detector, the GPIC detector also exploits the orthogonality of the in-cell user transmissions in the IS–95 downlink.

In the following development, we consider an approach similar to that described in [21] where a conditional maximum likelihood detector was developed by relaxing the maximum likelihood criterion for a set of undesired symbols. Suppose temporarily that the IS–95

downlink receiver has perfect knowledge of $\hat{\bar{\boldsymbol{b}}}_{\mathsf{OPT}}$, the jointly optimum symbol estimate of the users' symbols in cells $2, \ldots, M$. In this case, we showed in Section IV that $\hat{\boldsymbol{b}}^{[1]} = \mathrm{sgn}(F(\hat{\bar{\boldsymbol{b}}}_{\mathsf{OPT}}))$ is the jointly optimum estimate of the users' symbols in cell 1. Unfortunately, realistic receivers do not have access to the jointly optimum out-of-cell symbol estimates in general, but we are compelled to ask the following question: What if the receiver formed some low-complexity estimate $\hat{\bar{\boldsymbol{b}}}$ of $\bar{\boldsymbol{b}}$ and we let $\hat{\boldsymbol{b}}^{[1]} = \mathrm{sgn}(F(\hat{\bar{\boldsymbol{b}}}))$? In fact, consider the lowest complexity estimate of $\bar{\boldsymbol{b}}$: conventional matched filter estimates where $\hat{\bar{\boldsymbol{b}}}_{\mathsf{MF}} = \mathrm{sgn}(\mathrm{Re}(\bar{\boldsymbol{A}}^H \bar{\boldsymbol{y}}))$. Then

$$\begin{aligned} \hat{\boldsymbol{b}}^{[1]} &= \mathrm{sgn}(F(\hat{\bar{\boldsymbol{b}}}_{\mathsf{MF}})) \\ &= \mathrm{sgn}\left(\mathrm{Re}\left[\boldsymbol{A}^{[1]H}(\boldsymbol{y}^{[1]} - \boldsymbol{p}^{[1]}) - \sum_{m=2}^{M} \boldsymbol{H}^{[1,m]} \hat{\boldsymbol{b}}_{\mathsf{MF}}^{[m]}\right]\right) \end{aligned}$$

but since $\boldsymbol{H}^{[1,m]} = \boldsymbol{A}^{[1]H} \boldsymbol{R}^{[1,m]} \boldsymbol{A}^{[m]}$ then

$$\hat{\boldsymbol{b}}^{[1]} = \mathrm{sgn}\left\{\mathrm{Re}\left[\boldsymbol{A}^{[1]H}\left((\boldsymbol{y}^{[1]} - \boldsymbol{p}^{[1]}) - \sum_{m=2}^{M} \boldsymbol{R}^{[1,m]} \boldsymbol{A}^{[m]} \hat{\boldsymbol{b}}_{\mathsf{MF}}^{[m]}\right)\right]\right\}. \tag{8}$$

It is evident from this last expression that a detector using (8) forms decisions by subtracting the estimated out-of-cell cochannel interference from the matched filter inputs (minus the known pilot terms) corresponding to the users in cell 1. When this operation is performed on all of the base stations it is called parallel interference cancellation (first called multistage detection in [22]) and, since the interference cancellation is performed over groups of users, we coin the name Group Parallel Interference Cancellation for this detector. We can extend this idea to write the following expression for the GPIC detector of base station m as

$$\hat{\boldsymbol{b}}^{[m]} = \mathrm{sgn}\left\{\mathrm{Re}\left[\boldsymbol{A}^{[m]H}\left((\boldsymbol{y}^{[m]} - \boldsymbol{p}^{[m]}) - \sum_{m' \neq m} \boldsymbol{R}^{[m,m']} \boldsymbol{A}^{[m']} \hat{\boldsymbol{b}}_{\mathsf{MF}}^{[m']}\right)\right]\right\}$$

where $\hat{\boldsymbol{b}}_{\mathsf{MF}}^{[m']} = \mathrm{sgn}(\mathrm{Re}(\bar{\boldsymbol{A}}^{[m']H} \boldsymbol{y}^{[m']}))$. Assembling the symbol estimates into a $K(2L+1)$ vector containing all of the users' bits in the multi-cell system, we can write a a simple expression for the GPIC detector as

$$\hat{\boldsymbol{b}}_{\mathsf{GPIC}} = \begin{bmatrix} \hat{\boldsymbol{b}}^{[1]} \\ \vdots \\ \hat{\boldsymbol{b}}^{[M]} \end{bmatrix} = \mathrm{sgn}\left\{\mathrm{Re}\left(\boldsymbol{A}^H\left[(\boldsymbol{y} - \boldsymbol{p}) + (\boldsymbol{I} - \boldsymbol{R})\boldsymbol{A}\hat{\boldsymbol{b}}_{\mathsf{MF}}\right]\right)\right\}.$$

We note that although it is certainly possible to perform GPIC detection in batch where all $K(2L+1)$ symbols are first estimated with the conventional matched filter detector and stored prior to calculation of the GPIC symbol estimates, it is also possible to implement the GPIC detector with a decision delay proportional to K.

VI. Simulation Results

In this section we compare the performance of the optimum, GPIC, and conventional matched filter detectors via simulation. We examine a scenario where a nonsubscribing downlink receiver (e.g. an eavesdropper) is listening to IS–95 downlink transmissions in the simple cellular system shown in Figure 3 with $B = 2$ base stations and $K_1 = 2$ and $K_2 = 2$ users in each cell. The subscribing users in the system are represented by circles and our downlink receiver is represented by a square with an antenna symbol. We evaluate the quality of reception at the receiver from both base stations as the receiver moves on the dashed line from point a to point b.

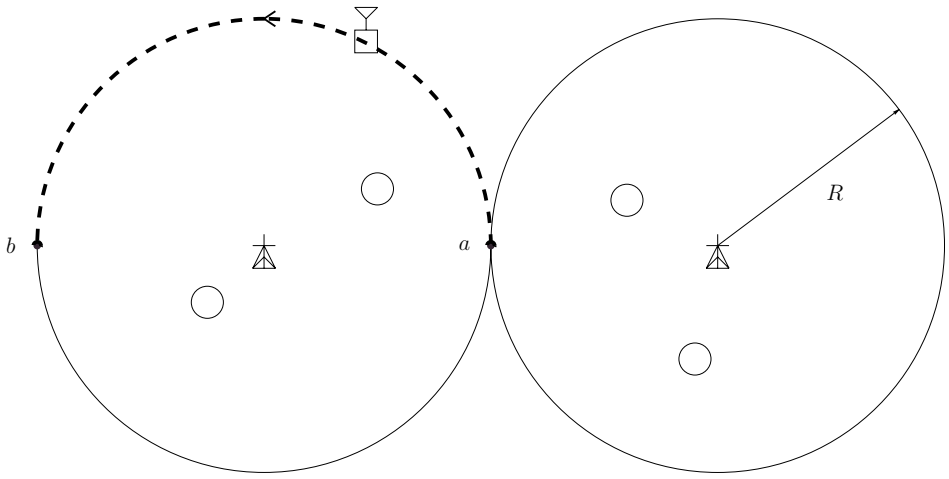

Fig. 3. Simple two base station IS–95 cellular system with cells of radius R and centered base stations.

The propagation channels between the base stations and the eavesdropping receiver are assumed to be single-path with random received phases uniformly distributed in $[0, 2\pi)$. Asynchronism offsets between the base station transmissions are also assumed to be uniformly distributed. User powers, phases and delays are assumed to be time invariant over the duration of the receiver's observation. We assume the user positions to be uniformly

distributed within the cell. This assumption combined with IS–95 downlink power control implies that the user amplitudes observed at the eavesdropper are also random. The distribution of the user amplitudes is derived in the Appendix under similar path-loss modeling assumptions as the uplink study in [23], [24].

Figure 4 shows the bit error rate of the optimum (denoted as "OPT"), GPIC, and conventional matched filter (denoted by "MF") detectors for a user in the first cell[2] averaged over the user positions, delays, phases, amplitudes, and PN-codes. The single-user error probability (denoted as "SU") is also shown for comparison. Note that, in this simulation, the distance to the desired base station is fixed and the out-of-cell cochannel interference is decreasing as we move the eavesdropper toward position b and away from base station 2. Figure 5 shows the results of the same simulation for a user in the second cell In this case the eavesdropper is moving away from the desired base station and remaining at a fixed distance from the interfering base station.

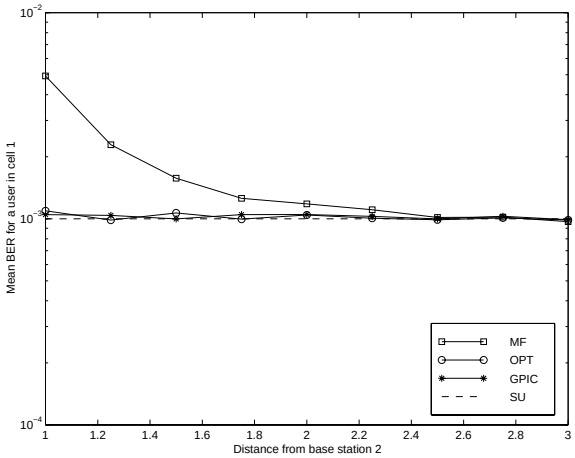

Figure 4: Averaged bit error rate for a downlink transmissions in cell 1.

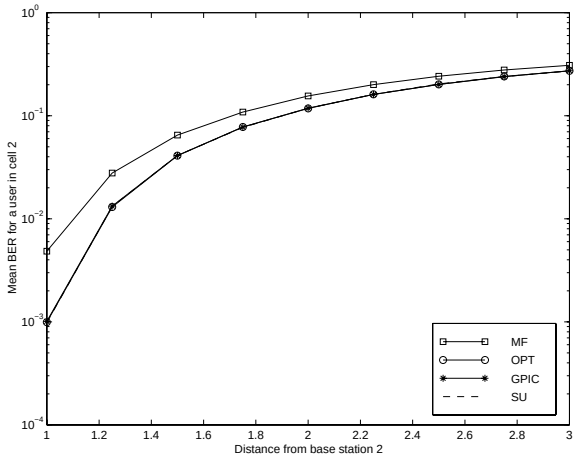

Figure 5: Averaged bit error rate for a downlink transmissions in cell 2.

Figure 4 shows that the conventional matched filter detector performs well when the eavesdropper is listening to a downlink transmission from base station 1 in a position distant from base station 2. However, because of its near-far susceptibility, the matched filter detector performs poorly when the eavesdropper attempts to extract weak downlink transmissions from strong out-of-cell cochannel interference. Figures 4 and 5 show that

[2]The first cell denotes the cell on the left of Figure 3 and the second cell denotes the cell on the right of Figure 3.

the GPIC detector does not suffer from this problem and actually exhibits performance indistinguishable from the optimum detector in these examples. These results suggest that the GPIC detector may offer near-optimum eavesdropping performance over a wide range of out-of-cell cochannel interference powers with the most benefit in severe out-of-cell cochannel interference environments.

VII. On-Air Data

This section compares the performance of the GPIC and conventional matched filter detectors on one snapshot of on-air measured data[3] from an active IS–95 cellular system. One 45.6ms snapshot of IS–95 downlink measured data was gathered with an omnidirectional antenna. The received waveform was sampled at twice the chip rate to yield a data file with 112000 samples corresponding to 875 (coded) symbol periods. The results of a base station pilot survey on this data are shown in Figure 6.

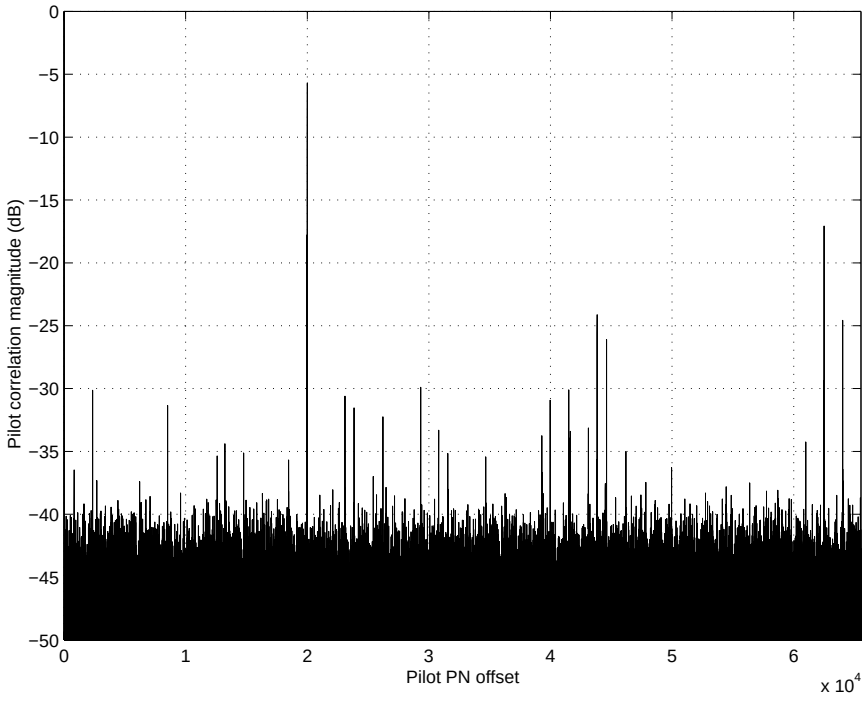

Fig. 6. Base station pilot survey for IS–95 on-air data.

[3]The authors would like to thank Rich Gooch, Mariam Motamed, and David Chou of Applied Signal Technologies, Sunnyvale, CA, for providing us with this data and also for their assistance in testing the algorithms developed in this paper.

Throughout this section, base station 1 denotes the base station with the strongest pilot as seen at PN-offset 20000 in Figure 6. Base station 2 denotes the second strongest base station at PN-offset 62500. The powers of each active Walsh channel at the output of their respective matched filter detector, for both base station 1 and base station 2, are given in Tables I and II. It can be seen that the power of the pilot (Walsh channel 0) from base station 1 is approximately 11dB higher than the pilot from base station 2, hence our receiver is positioned close to base station 1 and relatively distant from base station 2. The remaining base stations seen in Figure 6 are ignored in the following development for clarity.

Walsh Channel	% of BS1 transmit power	% of total received power
0	55.6	45.3
1	19.4	15.8
12	4.5	3.6
32	4.6	3.8
63	15.9	13.0
Total	100	81.4

TABLE I

Base station 1 active Walsh channels.

A. Conventional Matched Filter Detection

In this section we qualitatively examine the soft outputs of the conventional matched filter detector for base stations 1 and 2. The matched filters are obtained by estimating the impulse response of the combined propagation channel and pulse shaping filters via pilot correlation and convolving this impulse response with the appropriate combined Walsh and PN-codes for each active user in the system. Although Rake detection is not used, the matched filter detector considered in this section automatically includes coherent multipath combining since it incorporates the estimated impulse response of the propagation channel.

Figure 7 shows a histogram of the matched filter outputs for the active Walsh channels

Walsh Channel	% of BS2 transmit power	% of total received power
0	54.5	3.2
1	18.5	1.1
20	17.0	1.0
32	5.2	0.3
34	4.8	0.3
Total	100	5.9

TABLE II

Base station 2 active Walsh channels.

of base station 1. Figure 7 clearly shows that the eye is open for all of the active channels and implies that one could expect that these users' decoded symbols would have very low probability of error. In addition to the strong pilot channel at Walsh code 0, there is a strong paging channel at Walsh code 1, a relatively weak sync channel at Walsh code 32, and two traffic channels of disparate power at Walsh codes 12 and 63. Qualitatively, matched filter detection appears to be adequate for downlink reception of this base station.

Figure 8 shows a histogram of the matched filter outputs for the active Walsh channels of base station 2. Figure 8 clearly shows that, unlike the transmissions from base station 1, all of the channels from base station 2 are highly corrupted by interference (including out-of-cell cochannel interference from base station 1, other base stations, and "unstructured" noise sources). The eye is closed for all Walsh channels, implying that subsequent channel decoding may be unreliable.

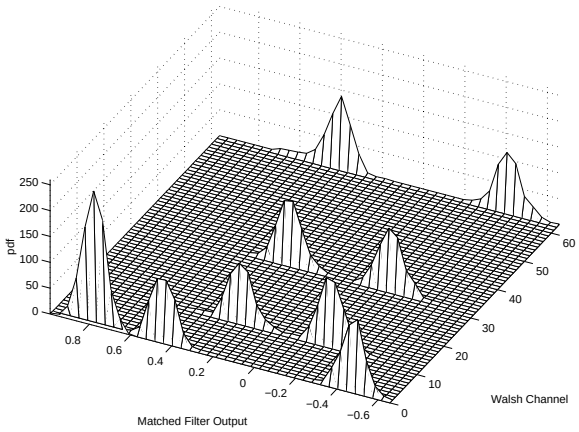

Figure 7: Histograms of MF outputs by Walsh channel for base station 1.

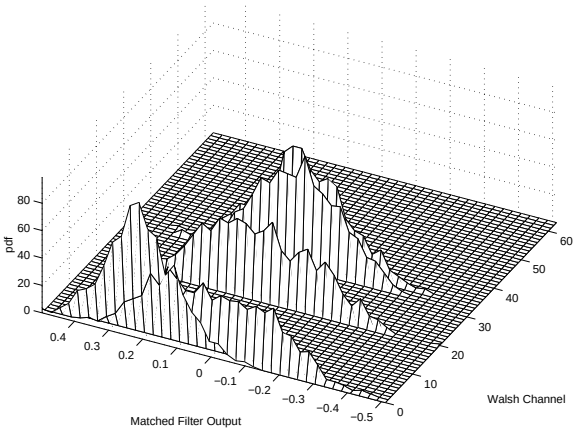

Figure 8: Histograms of MF outputs by Walsh channel for base station 2.

B. GPIC Detection

In this section we qualitatively examine the soft outputs of the GPIC detector for base stations 1 and 2. The matched filter outputs generated in the prior subsection are passed through a hard decision device and then respread by the combined impulse response of the appropriate Walsh codes, PN-codes, and estimated pulse-shaping and propagation channel impulse responses. The waveforms are then scaled and rotated according to each user's estimated amplitude and phase.

Figure 9 shows the histogram of the matched filter outputs by Walsh channel of base station 1 after subtraction of the estimated interference from base station 2. There is little noticeable change from the results in Figure 7 since the out-of-cell cochannel interference from base station 2 is very weak with respect to the transmission of base station 1 and interference cancellation has little effect.

Figure 10 shows the histogram of the matched filter outputs by Walsh channel of base station 2 after subtraction of the estimated interference from base station 1. The performance improvement is significant with respect to the conventional matched filter results in Figure 8. Channels 1 and 20 appear to be much cleaner and channels 32 and 34 are beginning to exhibit troughs in the middle of their histograms indicating improved detection quality. The pilot channel is also significantly cleaner.

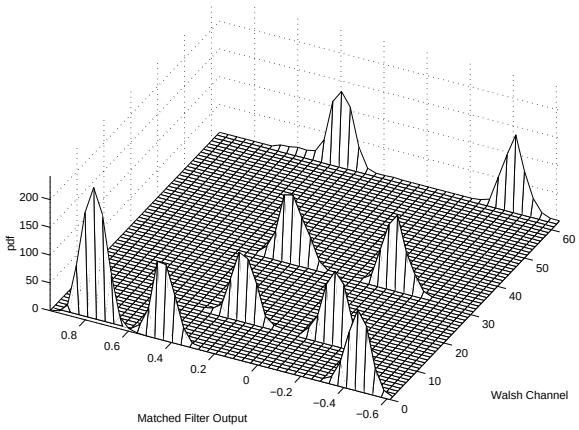

Figure 9: Histograms of GPIC outputs by Walsh channel for base station 1.

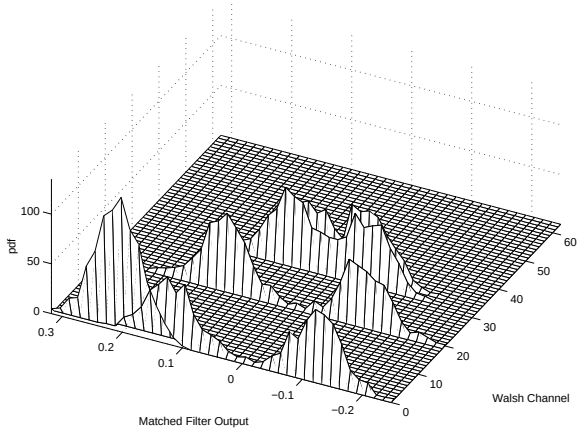

Figure 10: Histograms of GPIC outputs by Walsh channel for base station 2.

The results in this section agree with the simulation results in Section VI and suggest that the GPIC detector may not offer much performance improvement when detecting strong signals in the presence of weak out-of-cell cochannel interference. On the other hand, comparison of Figures 8 and 10 show that significant performance improvements are possible for a downlink receiver attempting to extract weak signals from strong out-of-cell cochannel interference.

VIII. Conclusions

In this paper we investigated nonlinear multiuser detection for improving the performance of IS–95 downlink reception. We used the orthogonality of the in-cell users of the IS–95 downlink to develop a reduced complexity optimum detector with exponentially lower complexity than the brute-force optimum detector under the assumption that the propagation channels between the base stations and the receiver were single-path. Examination of the properties of the reduced complexity optimum detector led to the development of the suboptimum, low-complexity GPIC detector. The GPIC detector does not require any form of subspace tracking, matrix inversions, or exhaustive searches for global maxima. Simulations and experiments with on-air IS–95 downlink data showed that the GPIC detector offers the greatest performance improvements when detecting weak desired signals in the presence of strong out-of-cell cochannel interference. Although this scenario would be unusual for a subscribing user in an IS–95 cellular system, a nonsubscribing

user such as an eavesdropper may derive the greatest benefit from GPIC detection. Our results also suggest that subscribing users that use GPIC detection can achieve an acceptable quality of service with less base station transmit power which results in less induced cochannel interference on out-of-cell users in the system.

Appendix: Received Power Distribution

In this appendix, we derive the received user power distribution for transmissions to users in the m^{th} cell observed by a receiver positioned at a deterministic distance $d^{(m)} \in (0, \infty)$ from the m^{th} base station. We impose the following assumptions:

- Each base station is located in the center of its circular cell of radius R.
- Each user's position is uniformly distributed in their cell and is independent of other user positions. The k^{th} user's distance from base station m is denoted by $d^{(m,k)} \in (0, R]$.
- Perfect power control is maintained between each base station and its users such that the power received is identical for all users within the cell.
- The ratio of received to transmitted power obeys a simple path loss model $1/d^{2\lambda}$ where d is the distance separating the transmitter and receiver, and λ is the path loss exponent.

The circular shape of each cell and the users' uniformly random positions imply that the cumulative distribution function of the $(m,k)^{\text{th}}$ user's distance from the m^{th} base station, denoted as $d^{(m,k)}$, is equal to the ratio of the area of 2 circles,

$$F_{d^{(m,k)}}(x) = P(d^{(m,k)} \leq x) = \begin{cases} (x/R)^2 & x \in [0, R], \\ 0 & \text{otherwise.} \end{cases}$$

The pdf of $d^{(m,k)}$ follows directly as

$$f_{d^{(m,k)}}(x) = \frac{\partial}{\partial x} F_{d^{(m,k)}}(x) = \begin{cases} 2x/R^2 & x \in [0, R], \\ 0 & \text{otherwise.} \end{cases}$$

IS–95 downlink power control leads to random realizations for the user amplitudes observed at a deterministically positioned receiver. The received power ratio (deterministically positioned receiver to randomly positioned user) may be expressed as

$$\Psi = \frac{\Pi^{(m)}}{\Pi^{(m,k)}} = \frac{\Pi^{(m)}/\Pi_t}{\Pi^{(m,k)}/\Pi_t} = \frac{(d^{(m,k)})^{2\lambda}}{(d^{(m)})^{2\lambda}}$$

where $\Pi^{(m)}$, $\Pi^{(m,k)}$, and Π_t denote the power of the m^{th} base station observed at the eavesdropper, the power of the m^{th} base station observed at the $(m,k)^{\text{th}}$ user, and the power transmitted by the m^{th} base station, respectively. To find the cumulative distribution of Ψ, we note that $F_\Psi(x) = P(\Psi \leq x) = P((d^{(m,k)})^{2\lambda}/(d^{(m)})^{2\lambda} \leq x) = F_{d^{(m,k)}}(d^{(m)}x^{1/2\lambda})$ hence

$$F_\Psi(x) = \begin{cases} (d^{(m)}/R)^2 x^{1/\lambda} & x \in [0, (d^{(m)}/R)^{-2\lambda}], \\ 0 & \text{otherwise} \end{cases}$$

and the pdf of Ψ follows directly as

$$f_\Psi(x) = \begin{cases} \lambda^{-1}(d^{(m)}/R)^2 x^{(1-\lambda)/\lambda} & x \in [0, (d^{(m)}/R)^{-2\lambda}], \\ 0 & \text{otherwise.} \end{cases}$$

This pdf is used to generate the random amplitude realizations used for the simulation results in Section VI.

References

[1] Telecommunications Industry Association, *Mobile Station – Base Station Compatibility Standard for Dual-Mode Wideband Spread Spectrum Cellular Systems IS–95A*. Washington, DC: TIA/EIA, 1995.

[2] R. Kohno, R. Meidan, and L. Milstein, "Spread spectrum access methods for wireless communications," *IEEE Communications Magazine*, vol. 33, pp. 58–67, January 1995.

[3] A. Klein, "Data detection algorithms specially designed for the downlink of CDMA mobile radio systems," in *1997 IEEE 47th Vehicular Technology Conference: Technology in Motion*, vol. 1, (Phoenix, AZ), pp. 203–7, May 4-7, 1997.

[4] I. Ghauri and D. Slock, "Linear receivers for the DS-CDMA downlink exploiting orthogonality of spreading sequences," in *Conference Record of the Thirty-Second Asilomar Conference on Signals, Systems, and Computers*, vol. 1, (Pacific Grove, CA), pp. 650–4, November 1-4, 1998.

[5] C. Frank and E. Visotsky, "Adaptive interference suppression for direct-sequence CDMA systems with long spreading codes," in *Proceedings of the 36th Annual Allerton Conference on Communications, Control and Computing*, (Monticello, IL), pp. 411–20, September 23-25, 1998.

[6] S. Werner and J. Lilleberg, "Downlink channel decorrelation in CDMA systems with long codes," in *1999 IEEE 49th Vehicular Techology Conference. Moving Into a New Millenium.*, vol. 2, (Houston, TX), pp. 1614–7, May 16-20, 1999.

[7] K. Hooli, M. Latva-aho, and M. Juntti, "Linear chip equalization in WCDMA downlink receivers," in *1999 Finnish Signal Processing Symposium*, vol. 1, (Oulu, Finland), pp. 1–5, May 31, 1999.

[8] K. Hooli, M. Latva-aho, and M. Juntti, "Multiple access interference suppression with linear chip equalizers in WCDMA downlink receivers," in *Proceedings of the IEEE Global Telecommunications Conference – Globecomm'99*, vol. 1A, (Rio de Janeiro, Brazil), pp. 467–71, December 5-9 1999.

[9] K. Hooli, M. Juntti, and M. Latva-aho, "Inter-path interference suppression in WCDMA systems with low spreading factors," in *1999 IEEE 50th Vehicular Techology Conference. Gateway to 21st Century Communications*, vol. 1, (Amsterdam, Netherlands), pp. 421–5, September 19-22, 1999.

[10] M. Heikkila, P. Komulainen, and J. Lilleberg, "Interference suppression in CDMA downlink through adaptive channel equalization," in *1999 IEEE 50th Vehicular Techology Conference. Gateway to 21st Century Communications*, vol. 2, (Amsterdam, Netherlands), pp. 978–82, September 19-22, 1999.

[11] K. Li and H. Liu, "Blind channel equalization for CDMA forward link," in *1999 IEEE 50th Vehicular Techology Conference. Gateway to 21st Century Communications*, vol. 4, (Amsterdam, Netherlands), pp. 2353–7, September 19-22, 1999.

[12] I. Chih-Lin, C. Webb, H. Huang, S. Brink, S. Nanda, and R. Gitlin, "IS-95 enhancements for multimedia services," *Bell Labs Technical Journal*, pp. 1:60–87, Autumn 1996.

[13] A. Weiss and B. Friedlander, "Channel estimation for DS-CDMA downlink with aperiodic spreading codes," *IEEE Transactions on Communications*, vol. 47, pp. 1561–9, October 1999.

[14] H. Huang, I. Chih-Lin, and S. ten Brink, "Improving detection and estimation in pilot-aided frequency selective CDMA channels," in *Proceedings of ICUCP 97 - 6th International Conference on Universal Personal Communications*, vol. 1, (San Diego, CA), pp. 198–201, October 12-16, 1997.

[15] H. Huang and I. Chih-Lin, "Improving receiver performance for pilot-aided frequency selective CDMA channels using a MMSE switch mechanism and multipath noise canceller," in *Proceedings of the 8th International Symposium on Personal, Indoor, and Mobile Radio Communications*, vol. 3, (Helsinki, Finland), pp. 1176–80, September 1-4, 1997.

[16] B. Zaidel, S. Shamai, and H. Messer, "Performance of linear MMSE multiuser detection combined with a standard IS-95 uplink," *Wireless Networks*, vol. 4, no. 6, pp. 429–45, 1998.

[17] B. Zaidel, S. Shamai, and S. Verdú, "Multi-cell uplink spectral efficiency of randomly spread DS-CDMA in Rayleigh fading channels," in *Proceedings of the 2001 International Symposium on Communication Theory and Applications*, (Ambleside, UK), July 2001.

[18] A. Viterbi, *CDMA: Principles of Spread Spectrum Communications*. Reading, MA: Addison-Wesley, 1995.

[19] Y. Steinberg and H.V. Poor, "Sequential amplitude estimation in multiuser communications," *IEEE Transactions on Information Theory*, vol. 40, pp. 11–20, January 1994.

[20] S. Verdú, *Multiuser Detection*. New York, NY: Cambridge University Press, 1998.

[21] C. Schlegel, S. Roy, P. Alexander, and Z. Xiang, "Multiuser projection receivers," *IEEE Journal on Selected Areas in Communications*, vol. 14, pp. 1610–1618, October 1996.

[22] M. Varanasi and B. Aazhang, "Multistage detection in asynchronous code-division multiple-access communications," *IEEE Transactions on Communications*, vol. 38, pp. 509–19, April 1990.

[23] A. McKellips and S. Verdú, "Eavesdropping syndicates in cellular communications," in *1998 IEEE 48th Vehicular Technology Conference*, vol. 1, (Ottowa, Canada), pp. 318–22, May 18-21, 1998.

[24] A. McKellips and S. Verdú, "Eavesdropper performance in cellular CDMA," *European Transactions on Telecommunications*, vol. 9, pp. 379–89, July/August 1998.